CZM analysis of secondary debondings induced by wedge splitting testing of multi-layer specimens

Nathan Lemartinel, Armelle Chabot, Eshan V. Dave, Laurent Gornet

CZM analysis of secondary debondings induced by wedge splitting testing of multi-layer specimens

N. LEMARTINEL[a], A. CHABOT[a], E. V. DAVE[b], L. GORNET[c]

a. Univ Gustave Eiffel, MAST-LAMES, nathan.lemartinel@protonmail.com, armelle.chabot@univ-eiffel.fr
b. University of New-Hampshire, eshan.dave@unh.edu
c. Ecole Centrale de Nantes, GEM, laurent.gornet@ec-nantes.fr

Résumé :

Dans des travaux de recherche antérieurs, l'essai de fendage par coin est utilisé pour caractériser à la rupture le collage des interfaces entre couches de matériaux de chaussée dont l'enrobé bitumineux, constituant principal de ces structures. Du fait de la grande taille des éprouvettes prélevées in situ, des interfaces secondaires correspondant à différentes couches sont présentes. Ces dernières se décollent lors de certains essais et perturbent les résultats. Ces ruptures d'interface sont modélisées par éléments finis (sous l'hypothèse des déformations planes) à l'aide de modèles de zone cohésive tels qu'existant dans les logiciels Abaqus et Cast3M. On montre que la prise en compte de rupture en mode II pour les interfaces secondaires explique en partie les résultats expérimentaux suivis par analyse d'images.

Abstract:

In previous research efforts to study interfaces between asphalt pavement layers, the wedge splitting test is used in order to characterize the fracture bond of interfaces between layers of pavement materials that are mainly made of bituminous concrete, the main structural component of pavements of these structures. Due to the large size of the specimens extracted from in-situ test-track sections, secondary layers exist in those specimens. These secondary bituminous concrete layers debond during some tests, perturbing the results. Finite element modelling of the Wedge splitting tests is conducted using the Cast3M and ABAQUS finite elements systems, with a cohesive zone fracture models for the interface. This research demonstrates that consideration of mode-II fracture response (in-plane shear) within the secondary layer interfaces can better explain the behavior observed in experiments.

Keywords: Cohesive Zone Model, Wedge Splitting Test, Debonding, Interface, Multi-layered, Bituminous Materials

1 Introduction

A pavement is a multi-layer structure composed in most cases of asphalt materials. These layers are bonded together with a thin layer of bitumen emulsion. A pavement is subject to periodic stresses, which corresponds to bending effect of the heavy moving loads (traffic) and climate-induced thermal and moisture cycles. This results in damage due to mechanical degradation. The bonding of asphalt concrete

layers is a key aspect to optimize the durability of the pavement structure [1]. To characterize the behavior of pavements' interfaces, the Wedge Splitting Test (WST) [2-4] (Figure 1) was used and adapted in the doctoral research by Gharbi [5] to test bituminous specimens extracted from pavement test sections. The WST, originally developed for evaluation of fracture behavior in cement concrete specimens, is an adaptation of the standard compact tension test (ASTM 1983). It consists in the opening and the fracturing of a specimen with a wedge with an angle small enough to get a steady fracture propagation along the interface. This test was used because it has ability to test large enough specimens and to capture the interface debonding between two materials with a stable crack propagation state in mode I of fracture process. It allows a precise monitoring such as the use of Digital Image Correlation technics.

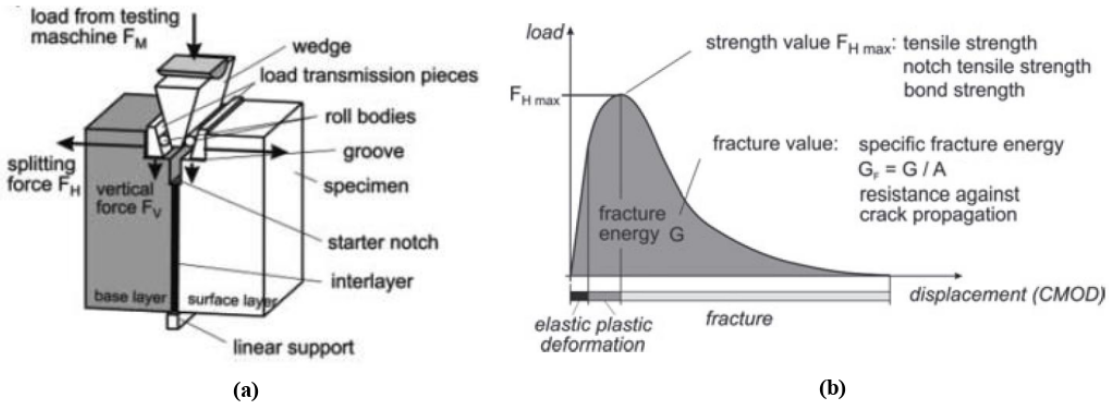

FIG. 1 – The Wedge Splitting Test (From [4]) (a) Specimen (b) Force - Displacement curve

Linked to the the ANR SolDuGri grant ANR-14-CE22-0019 (France) [6], different types of specimens have been extracted from an in-situ test trac [7-9]. In order to satisfy the minimum material heterogeneity volume sizes and the recommendations for the specimen dimensions, the average dimensions were of 200 ×250 ×150 mm3. Due to the large size of those heterogeneous specimens as well as typical process of constructing bituminous pavements in form of thin lifts, it is not possible to prepared specimen using only two material layers (with only one interface). This results in potential for secondary debonding between other sublayers as observed these above WST campaigns of 2 mm/min wedge displacement speed and ambient temperature of approximately 20°C (Figure 2) [6]. These multiple parasitic fractures affect the experimental results of the main interface that was intended to be characterized.

FIG. 2 – Example of secondary debonding during WST of extracted specimens coming from pavement test tract (from [5])

This paper presents finite element modeling of these WST experimental results using two types of cohesive zone model (CZM) approaches. First, these different CZM used to model the behavior of the interfaces are briefly discussed. Initial simulations are conducted under plane strain assumptions and assuming homogeneous properties between all WST sublayers. Taking into account the void ratio of each layer of the specimen to obtain their relative equivalent elastic modulus are then considered in the modeling to explain the secondary debonding that happened in some tests.

2 Cohesive Zone Models

A cohesive zone modelling approach has been developed to implement Griffith's energy based fracture response within a finite element modelling framework. The cohesive zone model typically uses interface elements of zero thickness that have softening response as a function of displacement jump along the nodes. Energy based measures along with intrinsic shape parameters are used to describe the softening response of cohesive zones elements. Due to use of displacement based criteria, cohesive zone elements are less sensitive to the mesh discretization and element size variations as compared to strain gradient based material degradation approaches, such as, continuum damage or smeared crack models. The cohesive zone is an intermediate zone between the fully separated crack edges and the undamaged material. Often in the cohesive zone, micro-cracks are appearing and coalescing to become the new crack tip. A CZM constitutive model describes, at a minimum, three fundamental material response aspects: stress levels at which material degradation initiates, maximum critical displacement along crack path at which material capacity is fully degraded (a macro crack is developed) and shape parameters that control energy dissipation rates and variations in the dissipation rate as function of fracture mode mixity. For tracking the extent of energy dissipation within cohesive zone, we define a damage local variable *d,* which evolves between 0 (material is undamaged) and 1 (rupture/macro-crack).
A cohesive zone model can be used in a finite elements code to model the propagation of a crack in a ductile material. We use and compare below two models. The Viscohinte model implemented into Cast3M software has been developed at the end of the 1990s for composite field application [10-11]. It has the advantage to take into account the damage and delay response of the materials as it occurs in bituminous material due to its viscoelastic behavior. The Viscohinte model involves 9 parameters. Assuming that the damage variable *d* affects all opening modes in the same way, the behavior of the interface is described below (1):

$$\begin{cases} \sigma_{13} = (1-d)k_s[U_1] \\ \sigma_{23} = (1-d)k_s[U_2] \\ \sigma_{33} = (1-d)k_n[U_3] \end{cases} \quad (1)$$

Where [Ui] are the relative displacements of each side of the interface, *kn* and *ks* are the traction and shear interface rigidities parameters. The thermodynamic forces combined to the damage variable are expressed such as (2) (where $\langle \dots \rangle_+$ represents the positive part):

$$Y_{d_1} = \frac{1}{2}\frac{{\sigma_{13}}^2}{k_s(1-d)^2}, Y_{d_2} = \frac{1}{2}\frac{{\sigma_{23}}^2}{k_s(1-d)^2}, Y_{d_3} = \frac{1}{2}\frac{{\langle\sigma_{33}\rangle_+}^2}{k_n(1-d)^2} \quad (2)$$

Thus the dissipated energy in this model is expressed by (3):

$$\Phi = \left(Y_{d_1} + Y_{d_2} + Y_{d_3}\right)\dot{d} \quad (3)$$

The damage variable is governed by an equivalent energy release rate function given in (4):

$$Y(t) = \left(Y_{d_3}{}^{\alpha} + \left(\gamma Y_{d_1}\right)^{\alpha} + \left(\gamma Y_{d_2}\right)^{\alpha}\right)^{\frac{1}{\alpha}} \quad (4)$$

Where γ is a coupling parameter and α a material parameter governing the damage evolution in mixed mode. The local damage evolution law is then defined as follows (5):

$$\begin{array}{c} if[d < 1 \text{and} Y < Y_R]: \\ \dot{d} = k\left\langle \omega\left(Y(t)\right) - d\right\rangle_+^m, \quad \omega\left(Y(t)\right) \leq 1 \\ else: \\ d = 1 \end{array} \quad (5)$$

With ω(Y(t)) a material function, called delamination function, defined by (6):

$$\omega(Y) = \left[\frac{n}{n+1}\frac{\langle Y - Y_0\rangle_+}{Y_c - Y_0}\right]^n \quad (6)$$

The parameter *n* is a characteristic of the material, the larger n is, the brittler the interface. *Y0* and *Yc* are respectively the threshold damage energy and the critical damage energy. *k* and *m* are delay parameters, especially useful for viscoelastic or viscoplastic materials modeling. Finally, Y_R an energy corresponding to rupture expressed as (7):

$$Y_R = Y_0 + \frac{n+1}{n} d^{1/n}(Y_c - Y_0) \quad (7)$$

The other CZM used in this research is a bilinear CZM that has been tailored for bituminous materials by Song et al. [11]. This model utilizes a very high stiffness initial compliance portion of the force-crack opening displacement portion to minimize energy dissipation due to artificial compliance aspect of pre-embedded cohesive zone fracture elements. After the stresses within the cohesive zone elements reach material strength thresholds (traction strength for mode-I and shear strength for mode-II), a linear softening curve is adopted to provide relationship between stress transfer capacity of cohesive element and displacement jump along nodes perpendicular to the crack path. Dave and Behnia [12] have provided the relationship bilinear CZM and demonstrated its application for simulation of disk-shaped compact tension fracture test that is used for measurement of fracture properties of bituminous concrete.

3 CZM simulations applied to the WST

3.1 Identification and comparison of two CZM approaches

Linear elasticity is used to model the layers in the WST and a CZM to model the behavior of the interface. Two different meshes are done. The first one (1323 elements of degree 1) only models the main tested interface, assuming perfect bonding for the two secondary interfaces. This mesh with a reduced complexity allows a faster computation and is used to identify the parameters of the Viscohinte model. The second mesh (3071 elements of degree 1) models all of the three interfaces, allowing to take into account differences in modulus between the four layers and to model secondary debondings. In this

paper, the parameters of the Viscohinte model [11] remain the same for each interface, though it could be differentiated. These two meshes are displayed on Figure 3.

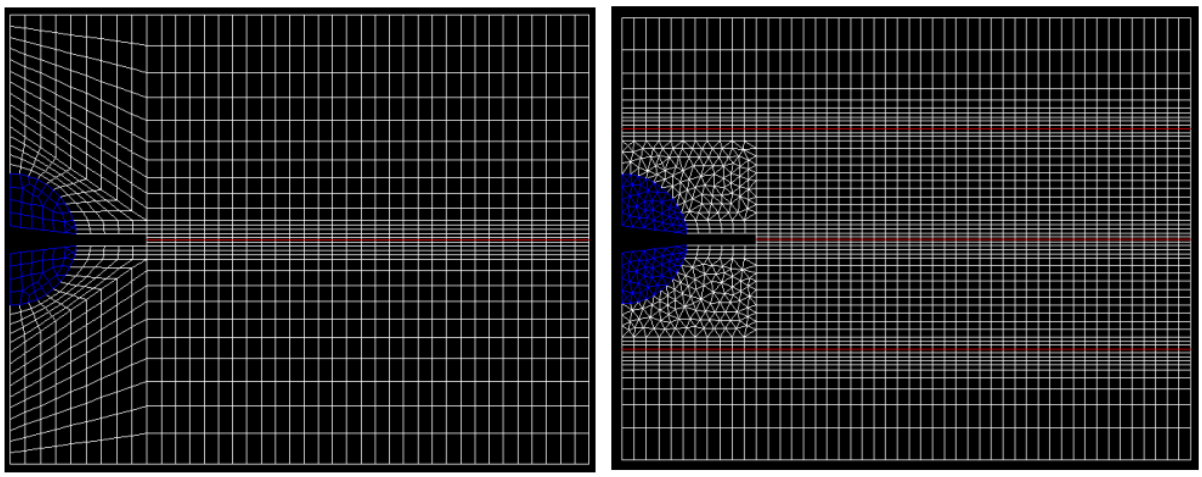

FIG. 3 - Cast3M meshes (a) Single interface (b) Triple interface

An identification of the Viscohinte parameters has been carried out by trial and error with the curve of an experimental test (called P8-8b specimen in [5]) where no perturbation was recorded. This will be used as a base set of parameters for the next attempts of fitting experimental curves. After several tests, it has been chosen to set some parameters of the Viscohinte model, which appeared not to be relevant for this simulation, to arbitrary values. ks is set to $kn/(2*(1+\nu))$, where $\nu = 0.35$ is the Poisson's ratio of asphalt concrete, Y_0 is set to 0, k is set to 1. α and γ are shear balance parameters, so as the crack of interest is propagating mainly in mode I, for now these are set not to take shear stresses into account. The remaining parameters are used as variables to fit the P8-8b curve. The selected values of the Viscohinte parameters are summarized in the Table 1.

Table 1 - Viscohinte parameters for the P8-8b fit

Parameter	kn (MPa/mm)	ks (MPa/mm)	Y_0 (N/mm)	Y_c (N/mm)	m	k	n	α	γ
Value	3000	$kn/(2*(1+\nu))$	0	43	1.25	1	0.1	1	0

The bilinear CZM from [13] was utilized within ABAQUS finite element analysis software to simulate WST. Similar trial and error process as used for Viscohinte model was conducted for the P8-8b specimen. The resulting fit and the fits achieved with the bilinear model on Abaqus are presented Figure 4. It is to be noted that the value of the G_F parameter (≈ 50 N/mm) of the bilinear model is closed to the value of Viscohinte's Y_C (≈ 43 N/mm).

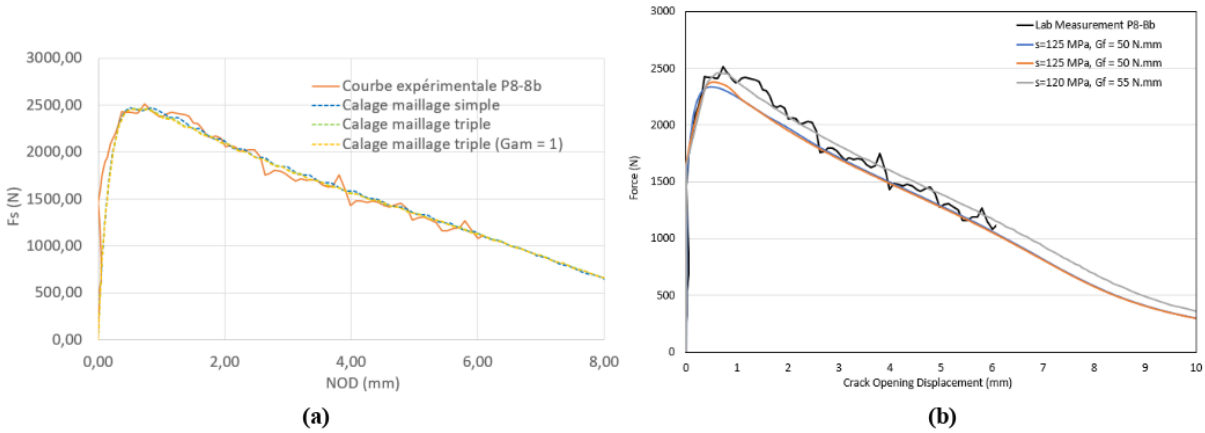

FIG. 4 - Fit of P8-8b experimental curve with (a) Viscohinte model (b) Bilinear model

3.2 Analysis to explain Secondary debonding occuring in some WST results

Compaction is done during the construction of a pavement so as to reach a precise void ratio in the asphalt concrete. This void ratio is one of a major parameters determining the properties of the material. Especially, the Young's modulus of asphalt concrete is very dependent on the void ratio [14]. This parameter is difficult to control precisely at industrial scale, so it has been suspected to be an important factor of the dispersion in the behaviors of the specimens. An attempt to model a test presenting a secondary debonding (called P8-6a specimen in Gharbi's PHD thesis [5]) and a comparison with the reference test P8-8b are made. Some measurement of the void ratio in specimens where secondary debondings occurred were done for each layer, and a great dispersion has been observed. The data of the void ratio into the layers of the P8-6a specimen was accessible, such as recommended in the SETRA-LCPC Technical Guide [14] 500MPa per point of compactness is assumed to estimate the Young's modulus in each layer of the specimen. The moduli approximated this way can be applied in the numerical model (Figure 5a), aside of the dimensions of the specimen. However, the void ratio of the P8-8b specimen's layers hasn't been measured. The moduli of this specimen are assumed to be all equal to 5000 MPa, as the Viscohinte parameter set is calibrated with this value. The second mesh on Cast3M with three interfaces is used to determine the influence of the secondary interfaces on the Force - Displacement curve. If the central tested interface undergoes mainly mode I fracture, the secondary interfaces are a priori subject to a more complex mix of mode I and II. Therefore, in order to activate mixed mode damaging on the interfaces with Viscohinte and evaluate the influence of shear damaging, γ is arbitrarily set to 1. Then α is noticed to have a great influence on the resulting curve. It is used along with the specimen dimensions and layers moduli to investigate different combinations. The resulting curves are displayed Figure 5.

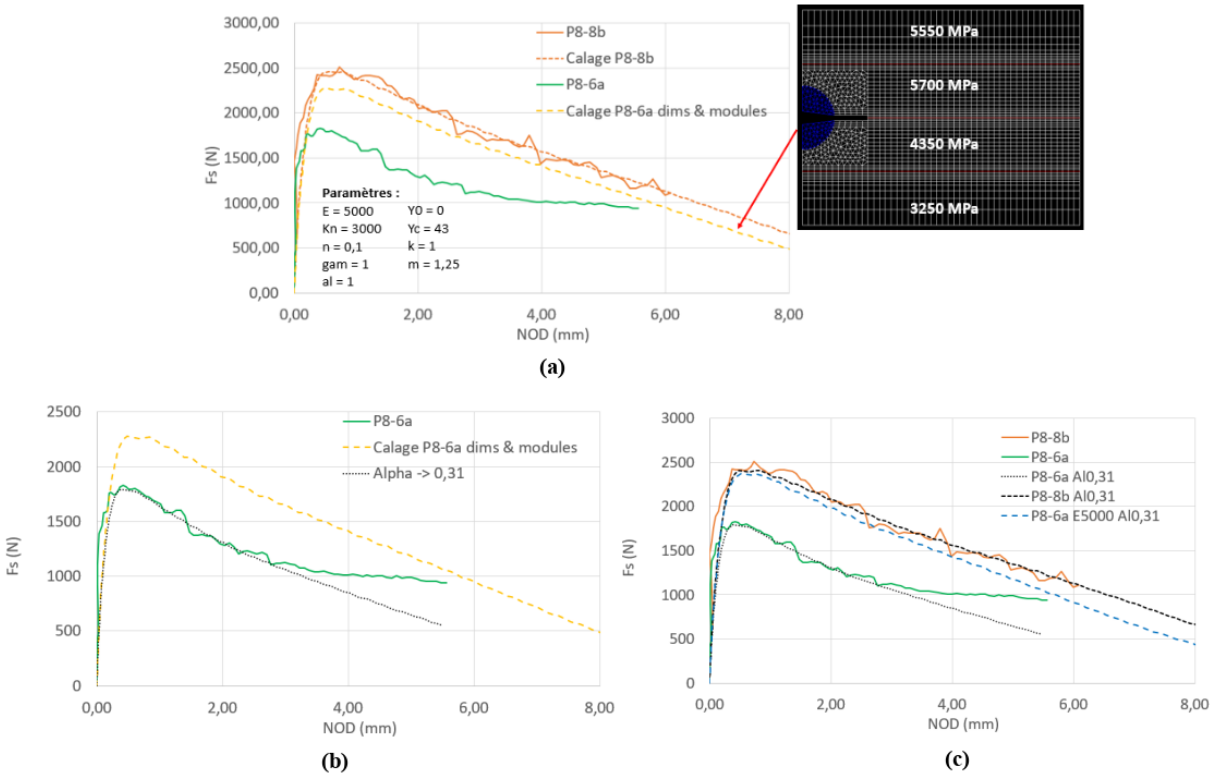

FIG. 5 - Influence of shear parameters on the fits of P8-8b and P8-6a tests with Viscohinte (a) effect of elastic modulus for layers (b) effect of parameters α and γ (c) numerical solutions fitted to experimental results

The Figure 5 shows the curves of two tests (solid lines) and several fits (dashed lines). The orange line is the experimental curve of the P8-8b specimen with no perturbation during the test, while the green one is the curve of the P8-6a specimen with a secondary debonding occurrence. The resulting curve of the identification of the Viscohinte parameters (with P8-8b dimensions, all layers' moduli equal to 5000 MPa and no shear parameters) is displayed in orange dashed line Figure 5a. The yellow dashed curve is obtained with the same simulation by setting the dimensions and moduli of P8-6a (still no shear). This curve doesn't fit at all the experimental P8-6a curve, so we can't explain the behavior of P8-6a with the parameter set given Table 1. However, conserving P8-6a dimensions and moduli, when γ is set to 1 and α to 0.31, the first part of the P8-6a experimental curve is well fitted, as shown with the thin dashed black line Figure 5b. Now the key result is displayed Figure 5c: the thick dashed black curve is obtained with shear parameters activated, replacing dimensions and moduli by P8-8b ones. The result is almost identical to no-shear simulations, this shows that shear parameters have very little influence when P8-8b dimensions and a modulus of 5000 MPa is selected. This result shows that we found a parameter set for the interfaces that allows to obtain a fit for both P8-8b and P8-6a curves. Only setting the dimensions and the moduli of the specimen is sufficient to obtain one curve or another. Furthermore, the blue curve is obtained with the dimensions of P8-6a by setting this time all layers' moduli to 5000 MPa. The curve becomes much closer to P8-8b experimental curve than P8-6a, proving that this is actually the moduli variation between layers that has a great influence on the resulting curve (as the average value of P8-6a moduli isn't different enough from 5000 MPa to explain the difference observed on the experimental curves). Finally, a last result is given Figure 6: the thin black line is obtained with P8-6a dimensions and moduli, except for one external layer where the modulus is set to 10 MPa to investigate the behavior of the specimen when this external layer has debonded. A flattening of the post-peak part of the resulting

curve can be observed, as we observe it on the experimental curve. This behavior isn't reproduced by the P8-6a fit Figure 5 and may be related to the complete debonding of the external layer.

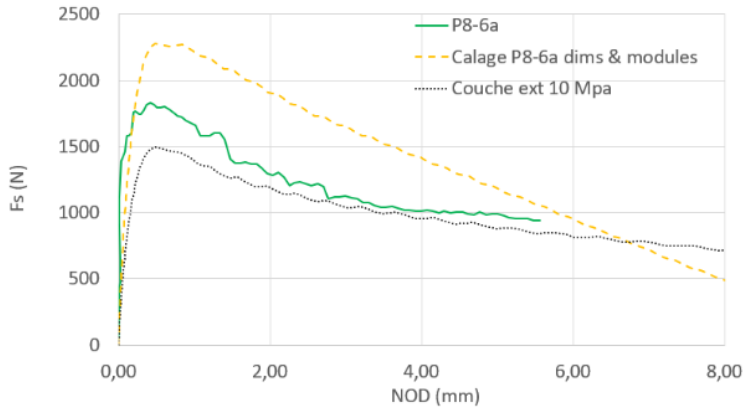

FIG. 6 - Influence of a complete debonding on the resulting curve

4 Conclusion

In this paper, two different Cohesive Zone Models (CZM) have been used [11,13] to highlight the behavior of interfaces between the layers in multilayered pavement specimens. These specimens were tested during the French SolDuGri ANR project by means of the Wedge Spitting Test (WST) [2-5]. Due to the large size of the specimens extracted from in-situ test-track sections, secondary layers exist in those. Under plane strain assumptions, first, the two CZM showed that all fracture processes were isolated along the primary tested interface. To explain delamination that occurs along secondary interfaces during some tests, the void ratio of each layer of the specimen were considered in the modeling. In the finite element software Cast3M, although a quite large number of Viscohinte parameters have to be determined with more care, the results tend to show that the moduli variations between layers of asphalt concrete has a huge impact on interfaces' failure by inducing shear stresses. A simpler bilinear CZM is able to also capture the primary interface failure in mode-I, this is demonstrated using analysis conducted with ABAQUS. As a next step, more comparisons between WST and CZM results will be done in order to enhance the fit and to better understand the role of each Viscohinte parameter.

References

[1] C. Petit, A. Chabot, A. Destrée, C. Raab, Recommendation of RILEM TC 241-MCD on Interface Debonding Testing in Pavements, Materials and Structures 51 (2018) 96
[2] E. K. Tschegg, Equipment and appropriate specimen shapes for tests to measure fracture values, AT No. 390328, Austrian Patent Office, Vienna, Austria, 1986
[3] E. Brühwiler, F.H. Wittmann, The wedge splitting test a new method of performing stable fracture mechanics tests. Engineering Fracture Mechanics 35(1–3) (1990) 117–125
[4] M. Jamek, E. L. Tschegg, R. Lugmayr, Mechanical and fracture–mechanical properties of geosynthetic reinforced asphalt systems, Fatigue & Fracture of Engineering Materials & Structures, 35 (2012) 648-657

[5] M. Gharbi, Caractérisation du collage des interfaces de chaussées par essais de rupture en mode I, Thèse, ECN, 2018
[6] M. L., Nguyen, C. Chazallon, M. Sahli, G. Koval, P. Hornych, D. Doligez, A. Chabot, Y. Le Gal, L. Brissaud, E. Godard, Design of reinforced pavements with glass fiber grids: from laboratory evaluation of the fatigue life and its FEM/DEM modelling to accelerated full-scale test, in: Chabot A., Hornych P., Harvey J., Loria-Salazar L. (eds), Proceedings of the 6th APT conference, LNCE 96, Springer, Cham, Switzerland, 2020, pp. 329-338, https://doi.org/10.1007/978-3-030-55236-7_34
[7] M. Gharbi, M.L. Nguyen, S. Trichet, A. Chabot, Characterization of the bond between asphalt layers and glass grid layer with help of a Wedge Splitting Test, in: A. Loizos, I. Al-Qadi, A. Scarpas (eds), Proceedings of 10th Int. Conf on Bearing capacity of Roads, Railway and Airfield (BCRRA2017), CRC Press, London, UK, 2017, pp. 1517-1524, doi: 10.1201/9781315100333-201
[8] M. Gharbi, M. L. Nguyen, A. Chabot, Characterization of Debonding at the Interface between Layers of Heterogeneous Materials coming from Roads, Proceedings of the 23ème Congrès Français de Mécanique, 2017, http://hdl.handle.net/2042/63293
[9] M. Gharbi, A.Chabot, J.L. Geffard, M. L. Nguyen, Interlaminar Mode-I Fracture Characterization Underwater of Reinforced Bituminous Specimens, in: Di Benedetto, H., Baaj, H., Chailleux, E., Tebaldi, G., Sauzéat, C., Mangiafico, S. (eds), Proceedings of the RILEM International Symposium on Bituminous Materials (ISBM 2020), RILEM Bookseries, 27, Springer, Cham., 2022, pp. 1119-1125, https://doi.org/10.1007/978-3-030-46455-4_142
[10] O. Allix, P. Ladeveze, A. Corigliano, Damage analysis of interlaminar fracture specimens, Composite Structures, 31(1) (1995) 61-74
[11] L. Gornet, D. Lévêque, L. Perret, Modélisation, identification et simulations éléments finis des phénomènes de délaminage dans les structures composites stratifiées, Mécanique Ind 1(3) (2000) 267–276
[12] S. H. Song, G. H. Paulino, W. G. Buttlar, A bilinear cohesive zone model tailored for fracture of asphalt concrete considering viscoelastic bulk material, Engineering Fracture Mechanics, 73(18) (2006) 2829-2848.
[13] E. V. Dave, B. Behnia, Cohesive zone fracture modelling of asphalt pavements with applications to design of high-performance asphalt overlays, Int J Pavement Eng 19(3) (2018) 319–337
[14] SETRA-LCPC, French Design Manual For Pavement Structures, Collection Guides techniques, Ministère de l'Equipement, des Transports et du Logement, France, 1997